

Rate Constants for the Trapping of Various Carbon-Centered Radicals by Nitroxides: Unimolecular Initiators for Living Free Radical Polymerization

W. G. Skene and J. C. Scaiano*

Department of Chemistry, University of Ottawa, 10 Marie Curie, Ottawa, Ontario, K1N 6N5 Canada

Nancy A. Listigovers, Peter M. Kazmaier, and Michael K. Georges

Xerox Research Center Canada, Mississauga, Ontario, L5K 2L1 Canada

Received October 20, 1999; Revised Manuscript Received April 6, 2000

ABSTRACT: The recapping kinetics of a series of unimolecular initiators for free radical polymerization were investigated. The rate constants for the trapping of various carbon-centered radicals were analyzed as a function of structurally different nitroxides in order to determine suitable candidates for living free radical polymerization (LFRP). The technique of laser flash photolysis was used to determine the trapping rate constants for the radicals in the presence of various amounts of nitroxide and to also gain insight into the properties of the LFRP process.

Introduction

Nitroxides have been extensively used for widespread applications in chemistry. These include the introduction of functionality¹ for synthetic purposes and reducing properties,^{2–5} and it may also be used as a protecting group⁶ that can be photochemically cleaved. The ability of nitroxides to trap carbon-centered radicals has been known for some time, and nitroxides were used as scavengers to inhibit polymerization or polymer degradation.^{7–14} The situation has recently been reversed, where nitroxides are now used to promote free radical polymerization in a controlled manner. Georges et al.^{15,16} found that these persistent radicals could be used to control polydispersity during the free radical polymerization process, where the lack of adequate molecular weight control has been a major drawback. The process, known as “living” free radical polymerization (LFRP),¹⁵ is characterized by low polydispersities, which represents an attractive advantage. The discovery of LFRP has drawn great interest recently, as free radical polymerization is more attractive, as less stringent requirements than for ionic polymerization are necessary.¹⁷ The incorporation of a nitroxide group also renders the polymer “living” as the thermally labile cap can be removed and polymerization resumed with the same or another monomer.

Unimolecular initiators have been introduced as an attractive advantage over in situ formed initiators. They offer the possibility of having a shelf-stable initiator available that can readily initiate polymerization producing the two relevant radicals in a stoichiometric ratio. More importantly, unimolecular initiators afford the means to study the key radical processes that occur during polymerization, as they can be considered as the first unit of the polymer. This mimetic feature allows the thermodynamic, kinetic, and other properties of LFRP to be examined with the added simplicity of working with small molecules.^{18–20} This is the primary reason for which unimolecular initiators have drawn a great deal of attention. Here the kinetics of radical

reactions of relevance to several new initiators have been examined. Laser flash photolysis (LFP) was used to determine the rates of radical trapping with structurally different nitroxides to identify candidates for unimolecular initiators and to gain insight into the influence of nitroxide structure and electronic factors on the LFRP process. In general, the candidates chosen to study thermally and photochemically decompose to give the propagating radical found in styrene and acrylate polymerization. The series of compounds shown in Chart 1 are conducive to investigating the influences of various structures upon the capping reaction associated with the LFRP process of styrene and methyl acrylate.

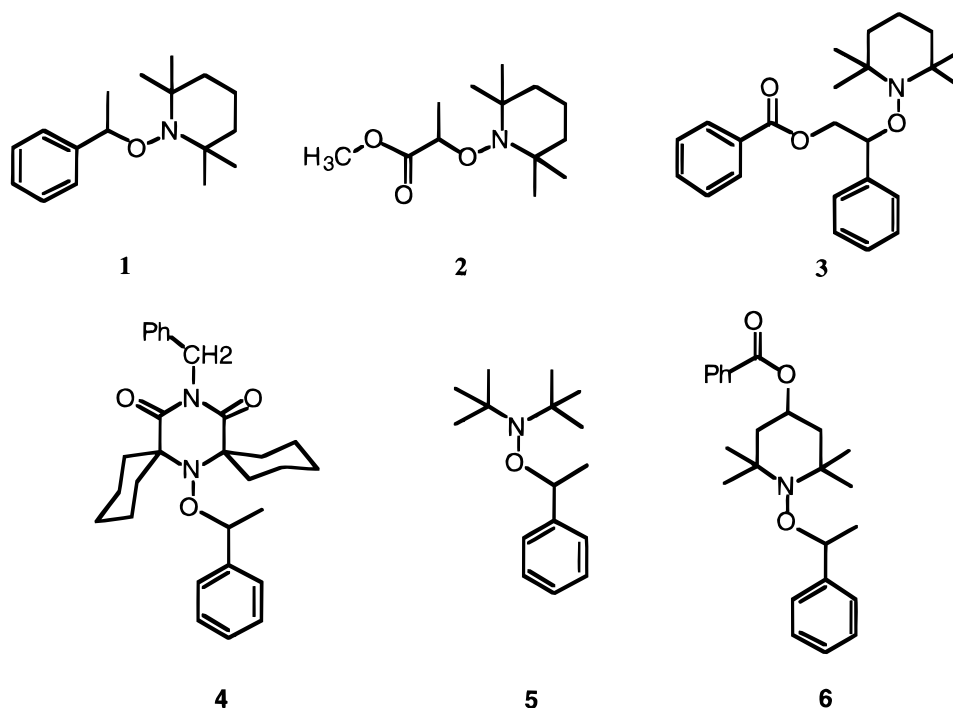
Experimental Section

An HPLC instrument equipped with a diode array absorption detector was used to determine the nitroxide concentrations immediately following LFP studies. A Zorbax C-18 reverse phase column (4.6 mm × 25 cm) with 85% methanol/15% water was used as eluent. Products formed after irradiation studies were analyzed with the same setup using LC-MS, yet the detection method was UV absorption at 254 nm coupled with an ESI mass spectrometer.

Rate constants were determined using the laser flash photolysis technique with nanosecond resolution. The laser system and the data processing after acquisition are similar to that previously reported.^{21,22} Excitation at 266 nm from a Continuum Nd:YAG Surelite laser (fourth harmonic, 10 mJ/pulse, ~6 ns) was used for direct photolysis of the photoinitiators. The 308 nm pulses from an excimer laser were also used in some experiments with other radical precursors. Moletron UV-24 nitrogen laser for 337 nm was used for work involving radical generation from di-*tert*-butyl peroxide and described elsewhere.^{7–9} All pulse durations are <10 ns and typical pulse energies between 5 and 50 mJ. Several methods for determining the rate constants were used (vide infra). In general, all samples were dissolved in spectroscopic grade acetonitrile, unless otherwise stated, and fully deaerated in a 7 × 7 mm² quartz Suprasil cell for a minimum of 20 min prior to use.

Synthesis of Initiators. The initiators used in this work either were the same as in earlier publications or were

Chart 1



prepared using the same methodology. Their identities were confirmed by NMR (^1H and ^{13}C) and mass spectrometry.

1-Phenyl-1-(2,2,6,6-tetramethylpiperidine-*N*-oxide)ethane (1). A 250 mL UV reactor vessel was charged with ethylbenzene (250 mL), 2,2,6,6-tetramethylpiperidine-*N*-oxyl (17.0 g, 109 mmol), and di-*tert*-butyl peroxide (23.0 mL, 18.3 g, 125 mmol). Oxygen was purged from the reaction vessel by bubbling argon through the solution, and then the product was irradiated at room temperature using a Conrad-Hanovia medium-pressure mercury vapor lamp with a 220 nm cutoff filter until the orange color of the nitroxide had disappeared (5 days). The reactor was discharged, and the residual ethylbenzene was removed by evaporation. Recrystallization from 2-propanol afforded colorless crystals in 63% yield. ^1H NMR (500 MHz, CDCl_3 TMS): δ 7.05–7.30 (m, 5H), 4.83 (q, 1H), 1.5 (s, 3H), 1.27 (m, 21H). ^{13}C NMR (300 MHz, CDCl_3): δ 145.8, 127.9, 126.7, 126.5, 83.0, 59.6, 40.3, 34.4, 34.1, 23.5, 20.3, 17.2. MS (EI): m/z (%) 156 (37), 142 (100), 123 (21), 114 (4), 105 (77), 104 (23), 77 (13), 69 (40), 56 (14), 55 (19), 41 (17). MS (ESI): m/z (%) 262 (5, $M + 1$), 157 (95), 126 (100), 125 (55), 121 (30), 105 (14), 82 (16), 69 (85), 57 (10), 42 (13).

2-(2,2,6,6-Tetramethylpiperidine-*N*-oxide)methylpropionate (2) was prepared as reported,²³ and its properties agreed well with the proposed structure.

1-Benzoyloxy-1-(2,2,6,6-tetramethylpiperidine-*N*-oxide)ethane (3) was prepared as reported in the literature.^{24,25}

1-Benzyl-3,3,5,5-dicyclohexyl-4-(1-phenylethoxy)piperazine-2,6-dione (4). Ethylbenzene (25 mL), BODAZ (5) (830 mg, 2.33 mmol), and di-*tert*-butyl peroxide (0.49 mL, 390 mg, 267 mmol) were combined, and the same procedure as **1** was followed. After the color had bleached (6 days), the solution was discharged and the residual ethylbenzene was removed by evaporation. Recrystallization from 2-propanol afforded colorless crystals in 78% yield. ^1H NMR (200 MHz, CDCl_3 TMS): δ 7.20–7.32 (m, 10H), 4.82 (q, 1H), 1.5 (d, 3H), 1.08 (s, 9H), 1.05 (s, 9H). ^{13}C NMR (300 MHz, CDCl_3): δ 157.2, 132.5, 128.3, 128.1, 127.9, 127.5, 127.1, 90.8, 82.5, 77.4, 77.0, 76.6, 43.8, 33.2, 25.9, 25.5, 22.4, 20.5. MS (EI): m/z (%) 355 (1), 339 (10), 297 (13), 249 (25), 209 (68), 178 (39), 122 (36), 105 (100), 91 (59), 77 (82), 51 (45).

1-Benzyl-3,3,5,5-dicyclohexyl-2-*N*-oxy-piperazine-2,6-dione (BODAZ). BODAZ was prepared by a procedure adapted from Ramey and Luzzi.²⁶ To a solution of 4-*N*-benzyl-4-azoglutarimide [prepared by the procedure of Ramey and Luzzi] (2.70

g, 8 mmol) in dichloromethane (75 mL) was added 3-chloroperoxybenzoic acid (99%) (2.76 g, 16 mmol). The temperature rose to 28 °C during the course of the addition. After 24 h, the precipitate was filtered off, and the lemon yellow solution was chromatographed on silica gel using hexane ethyl acetate (3%). The product was isolated as an orange syrup (2.01 g, 71%). MS (EI): m/z (%) 355 (26), 340 (100), 297 (28), 284 (12), 269 (39), 249 (26), 216 (19), 178 (36), 109 (15), 91 (57), 69 (29), 55 (9), 40 (39).

1-Phenyl-1-(*N,N*-di-*tert*-butyl-*N*-oxide)ethane (5). The previously described literature procedure was followed.²⁷

1-Phenyl-1-(4-benzoyloxy-2,2,6,6-tetramethylpiperidine-*N*-oxide)ethane (6). Ethylbenzene (25 mL), 4-benzoyloxy-2,2,6,6-tetramethylpiperidine-*N*-oxyl (262 mg, 10 mmol), and di-*tert*-butyl peroxide (2.3 mL, 1.83 g, 12.5 mmol) were combined, and a procedure similar to **1** was followed. After bleaching of the nitroxide color (6 days), the residual ethylbenzene was removed by evaporation. Flash chromatography with hexane–ethyl acetate (3%) gave a pale yellow syrup (yield 45%). ^1H NMR (200 MHz, CDCl_3 TMS): δ 8.0 (d, 2H), 7.21–7.97 (m, 8H), 5.24 (m, 1H), 4.79 (q, 1H), 1.50–1.97 (m, 4H), 1.47 (d, 3H), 1.23 (s, 1H), 1.16 (s, 1H), 1.06 (s, 1H), 0.68 (s, 1H). ^{13}C NMR (300 MHz, CDCl_3): δ 166.1, 145.3, 132.8, 130.6, 129.5, 128.3, 128.1, 126.9, 126.8, 126.7, 83.4, 76.9, 67.5, 60.3, 44.7, 34.4, 34.0, 23.3, 21.2, 21.0. MS (EI): m/z (%) 381 (26), 277 (35), 262 (17), 246 (10), 154 (17), 140 (143), 124 (77), 105 (100), 91 (8), 77 (51), 69 (11).

1-Benzoyl-2-phenylethane (7). Phenylethyl alcohol (1.04 g, 8.5 mmol) was dissolved in 30 mL of dichloromethane and cooled to 0 °C. To this solution was added 1.8 mL of triethylamine (12.9 mmol, 1.5 equiv) with a catalytic amount of *N,N*-dimethylaminopyridine. A solution of 1.2 mL of benzoyl chloride (10.3 mmol, 1.2 equiv) dissolved in dichloromethane was slowly added to the cooled solution. The resulting solution was allowed to warm to room temperature and stirred for 3 h. The reaction was judged completed by TLC. The reaction was quenched with a brine solution, and the organic layer was separated and further washed with brine. The organic layer was dried with magnesium sulfate, filtered, concentrated, and flash chromatographed with an eluent of 10% ethyl acetate/hexanes. This gave 1.95 g of **7** as a colorless oil (86%). ^1H NMR (200 MHz, CDCl_3 TMS): δ 8 (m, 2H), 7.4 (m, 8H), 4.5 (t, 2H), 3.1 (d, 2H). ^{13}C (300 MHz, CDCl_3): 166.5, 137.9, 132.9, 129.5, 128.9, 128.5,

Table 1. Rate Constants for the Reactions of Carbon-Centered Radicals with TEMPO^{8,9,36}

radical	solvent	k ($10^{-7} \text{ M}^{-1} \text{ s}^{-1}$)
$\text{C}_6\text{H}_5\text{CH}_2^\bullet$	acetonitrile	9.5
$\text{C}_6\text{H}_5\text{CH}_2^\bullet$	cyclohexane	41
$\text{C}_6\text{H}_5\text{CH}_2^\bullet$	isooctane	48
<i>n</i> -nonyl	acetonitrile	15
<i>n</i> -nonyl	cyclohexane	85
<i>n</i> -nonyl	isooctane	95

128.3, 126.6, 118.8, 65.5, 35.2. MS (FAB) m/z (%) 227 (20, M + 1), 132 (8), 105 (100), 77 (12), 57 (6). MS (EI): m/z (%) 105 (100), 91 (48), 77 (93), 65 (38), 51 (60). This molecule was employed as a precursor of a model radical (**8**) by hydrogen abstraction.

The ketone 2,4-diphenylpentane-2-one (**9**) was synthesized according to the literature procedure.²⁸

Results

The reactions of carbon-centered radicals (R^\bullet) with nitroxides have been examined in considerable detail by Ingold and co-workers.^{7–9} In general, these reactions are quite fast, but below the diffusion-controlled limit ($\sim 10^{10} \text{ M}^{-1} \text{ s}^{-1}$ for acetonitrile), and show a dependence on the polarity of the solvent, being slower in polar solvents. A few representative rate constants for TEMPO at room temperature are given in Table 1; they show that the rate constant for trapping is greater for aliphatic radicals. This is due primarily to the reduced stability of the radical.²⁹ We have examined the rate constants for trapping for the 1-phenylethyl radical as it is structurally similar to the propagating radical in the polymerization of styrene. Its trapping was examined as a function of various nitroxides to determine the influence of nitroxide radical structure and electronic contributions to the capping rate constant as found in the LFRP process. In addition to the styrene model radical, we also examined an aliphatic system that can be used as a model for acrylate systems. This model is represented by the methyl propionate initiator **2**. All the unimolecular initiators examined are found in Chart 1.

Initiators, such as those in Chart 1, among many others, can produce carbon-centered radicals and nitroxides in stoichiometric ratios, usually 1:1, by either thermal¹⁹ or photolytic decomposition.^{30,31} It is further assumed that the back-reaction involving combination of TEMPO or a nitroxide analogue with the carbon-centered radical provides a reasonable model for the recapping reaction involved in the reversible termination of nitroxide-regulated free radical polymerizations. In this sense, the back-reaction of the radicals derived from **1–6** can be expected to provide some insight into the dynamics of LFRP. We have examined a series of unimolecular initiators to determine the influence of nitroxide and carbon-centered radical structure on the back-reaction. This provides information pertaining to their capabilities as suitable candidates for LFRP.

In the simplest of cases, such as **1**, the decay of the radicals can be monitored under two distinct set of conditions with reference to the relative concentrations of the two radicals. The first case concerns two radicals that are produced in *identical* concentrations, as in reaction 1; then, their back-reaction should follow second-order kinetics. In general, k_2 (eq 2) is faster than k_3 (eq 3). Thus, self-reaction (e.g., benzyl radicals) tends to dominate when both radicals are present in equal concentrations. The example given illustrates the reac-

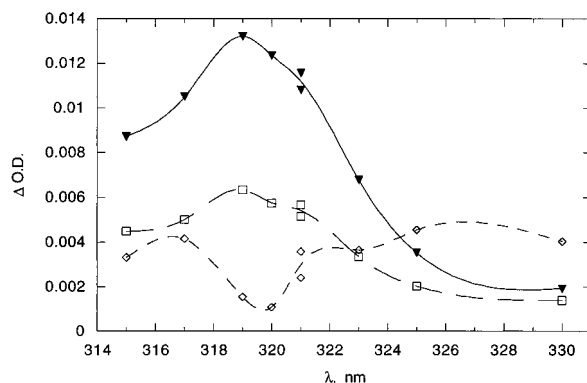
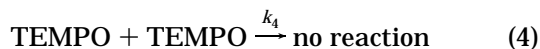
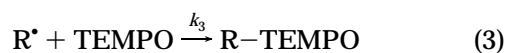
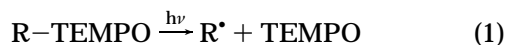


Figure 1. 1-Phenylethyl radical recorded in acetonitrile, recorded at 2.32 (▼), 8.88 (□), and 11.9 μs (◇, radical essentially gone) after laser pulse derived from direct photolysis of **1** with 266 nm excitation.

tion with TEMPO, but the same ideas apply to other nitroxides.



$$k_2 > k_3; \quad k_4 \sim 0$$

In the second case, when the persistent radical (nitroxide) is present in higher concentration, or if it accumulates during the experiment, reaction 3 dominates, and the process follows pseudo-first-order kinetics.^{32,33} This is a characteristic example of the Fischer–Ingold persistent free radical effect.^{34,35} Our experiments were carried out under these conditions (either by accumulation or addition of TEMPO) since they are more relevant to LFRP. The simplest way to achieve this is by direct photolysis of the initiators in the presence of various concentrations of added nitroxides in order to determine the pseudo-first-order rate constant for radical decay. However, some of the initiators in the series were not easily analyzed by this method, and other methods were required (vide infra). The rate constants measured in this study refer exclusively to the coupling reaction of the carbon-centered radical by the nitroxide shown in eq 3.

Initiators **1** and **3** have also been extensively studied^{7–9,16,18,24,36–41} as model compounds to probe the properties of LFRP. The initiator **1** is a relatively simple system that we have previously studied in terms of both thermodynamics^{19,30,31} and kinetics.^{42,43} Therefore, the rate constants derived from this initiator should shed some light into the kinetics of the polymerization of styrene systems. Upon laser excitation at 266 nm **1** undergoes the C–O bond fragmentation within the laser pulse ($\sim 10 \text{ ns}$)⁴⁴ and subsequently gives rise to the characteristic signal due to 1-phenylethyl radical with λ_{max} 319 nm (compare with benzyl radicals, λ_{max} 317 nm).⁴⁵ An expanded section of the relevant part of the transient spectrum is shown in Figure 1.

Carbon-centered radicals are rapidly scavenged by free nitroxides, and any residual nitroxide may influence the radical lifetimes. To avoid erroneous results arising

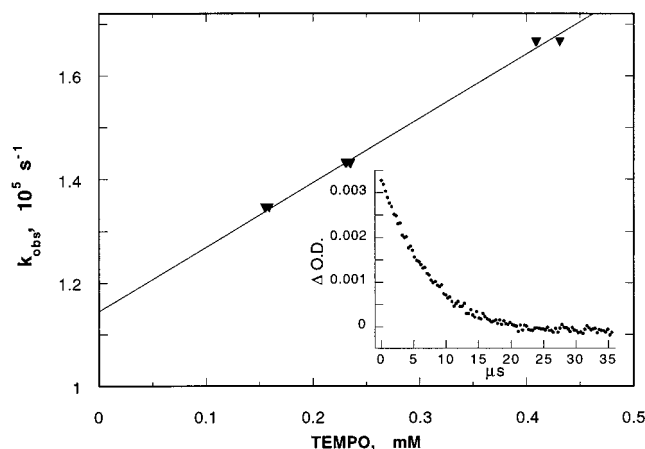


Figure 2. Quenching plot of 1-phenylethyl radical as a function of TEMPO concentration monitored at 319 nm in acetonitrile using the multiple cell method. Inset: decay of 1-phenylethyl radical also in acetonitrile monitored at 319 nm.

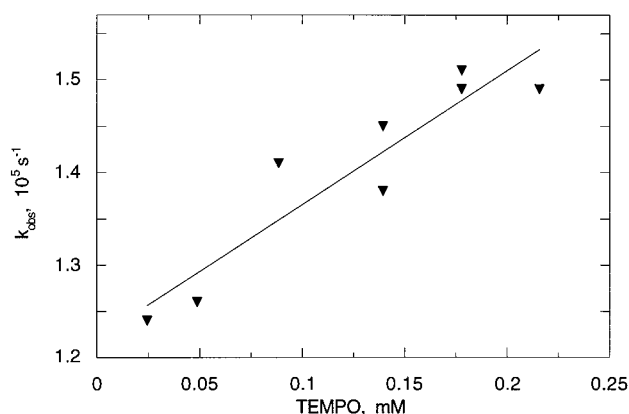


Figure 3. Quenching of 1-phenylethyl radical with TEMPO monitored at 319 nm in acetonitrile with the single cell method.

from this possibility, the nitroxide concentration was carefully determined by two methods. The two slightly different approaches were used in the determination of the rate constants. In one method (referred to as the "multiple cell" method), a series of samples were prepared containing equal concentrations of **1** and variable concentrations of added nitroxide. The lifetimes of the 1-phenylethyl radical were determined for each sample (a representative trace is shown in the inset of Figure 2), and the TEMPO concentration quenching plot is obtained by this method as seen in Figure 2, where k_{obs} is the reciprocal of the radical lifetime. Note that the values of k_{obs} correspond to $k_3[\text{TEMPO}]$ under strictly pseudo-first-order conditions. The desired k_3 value (eq 3) is obtained from the slope of various nitroxide concentrations as a function of k_{obs} , as shown in Figure 2.

In the second method (referred to as the "single cell" method), portions of a TEMPO stock solution were added to a single cell, and the radical lifetime was determined after each addition. A plot of this type is shown in Figure 3. At the end of the experiment the nitroxide concentration was determined on the basis of HPLC analysis. In the example of Figure 3, the nitroxide concentration was found to be 0.287 mM compared with 0.259 mM based on the sum of injected amounts. The difference (+11%) is consistent with some accumulation of TEMPO due to photolysis of **1** combined with minor HPLC calibration errors. The difference is

Table 2. Summary of Results Obtained by Quenching Various Carbon Centered radicals with various nitroxides in acetonitrile

initiator	radical gen method ^a	k_3 ($10^8 \text{ M}^{-1} \text{ s}^{-1}$)	other information
1	direct	1.24	multiple cells
	direct	1.34	single cell
2	direct	30	multiple cells
	direct	20	single cell
3	direct	(1.8)	single cell, <i>value uncertain</i> , see text
	probe	5.0	single cell
4	H-abstraction	0.95	mixed solvent with acetonitrile
	2,4-diphenylpropanone	2.0	
5	direct	0.71	
	2,4-diphenylpropanone	0.87	
6	direct	0.98	

^a See text for explanation of the various methods and radical generators.

relatively small and influences the rate constant only marginally. All measurements were performed under conditions where the radical decay followed first-order kinetics.

The values of k_3 obtained by both methods are given in Table 2 and lead to an average of $1.34 \times 10^8 \text{ M}^{-1} \text{ s}^{-1}$ for the 1-phenylethyl radical reacting with TEMPO. For the related benzyl radical, reported values are 4.8×10^8 and $9.5 \times 10^7 \text{ M}^{-1} \text{ s}^{-1}$ in isooctane and acetonitrile, respectively.^{8,9} It should be noted that in Ingold's work,⁷ which reported values of 1.6×10^8 and $1.9 \times 10^8 \text{ M}^{-1} \text{ s}^{-1}$ for the same system in isooctane, the radicals were generated by reaction of *tert*-butoxyl radical with toluene or the corresponding alkyl aromatic compound (vide infra). These reactions are not "instantaneous" sources of the radical⁴⁶ and may lead to somewhat slower apparent rate constants. We have previously determined²⁰ the rate of TEMPO trapping for the benzylic system in acetonitrile to be $2.1 \times 10^8 \text{ M}^{-1} \text{ s}^{-1}$ derived from an essentially instantaneous source of benzyl radicals. The rate constant measured supports the fact that the values for radicals derived from reactions of *tert*-butoxy radicals are somewhat slower due to the noninstantaneous nature of the radical forming process. The rate obtained here is somewhat slower partly because of the solvent polarity, as the solvent for the study is slightly more polar than that used by Ingold.⁹

Initiator **2** is an ideal model for probing the polymerization dynamics of acrylates and understanding the overall kinetics of polymerization of this aliphatic system in general. This is of interest because most research has focused primarily on styrene systems.^{14,47} The lack of published material on the acrylate systems has been mostly due to the difficulty in obtaining "living" qualities, although recently the Xerox and IBM groups have had some success in polymerizing acrylates.^{27,48–51} Only few examples^{10,52–55} have concentrated on analyzing the kinetics of nitroxides in the polymerization of acrylates. Therefore, **2** represents an ideal model compound to investigate the capping kinetics of acrylates in order to compare them to the LFRP for styrene-based systems.

The acrylate initiator **2** has no pendant aromatic group; this led us to anticipate that the radical generated by direct photolysis would be invisible to our LFP system. However, direct photolysis of **2** produces the transient spectrum as shown in Figure 4, and the maximum at 262 nm is ascribed to the methyl propionate radical.⁵⁶ The radical is not resonance stabilized

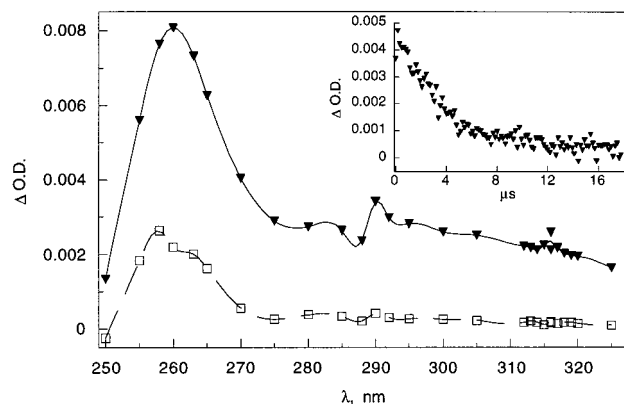


Figure 4. Transient spectrum of methyl propionate radical in acetonitrile recorded at 4.16 (▼) and 17.8 μ s (□) after initial laser pulse. Inset: decay of methyl propionate radical at 260 nm after excitation with 266 nm.

and is therefore expected to be blue-shifted compared to benzylic radicals.^{45,57} The methyl propionate radical has only a weak absorbance in the 260 nm region, which makes it difficult to analyze given the proximity of this wavelength to that of the intense 266 nm laser. TEMPO itself absorbs at this wavelength, thus effectively attenuating the xenon lamp monitoring beam employed in these experiments. Despite these difficulties, we were able to record the radical lifetime (inset in Figure 4) and spectrum with good signal-to-noise ratio. Therefore, quenching of the radical derived from **2** can be observed directly with TEMPO addition.

As was the case with **1**, two methods of determining the nitroxide concentration were used for **2**. Two determinations of the multiple cell method were done and lead to a rate constant in Table 2. All measurements were carried out under conditions where the decay followed first-order kinetics. However, in the absence of added nitroxide in fresh samples, the radical decay occurs with a mixture of first- and second-order kinetics. If the sample is exposed to a number of laser shots, the decay gradually becomes shorter, and first-order kinetics dominate as a result of TEMPO accumulation. In a preliminary experiment, we examined a sample in this fashion until we observed that a single exponential could easily fit the decay. HPLC analysis of this sample served to guide us in order to employ adequate concentrations of TEMPO, i.e., high enough to fit first-order kinetics yet low enough to minimize problems due to competitive light absorption by TEMPO. The results using the multiple cell approach are shown in Figure 5 lead to $k_3 = 3.0 \times 10^9 \text{ M}^{-1} \text{ s}^{-1}$. These measurements were far more difficult than those were for **1** and probably incorporate errors as large as $\pm 30\%$.

Attempts to measure this system with the single cell method led to complications as indicated by systematic negative intercepts in plots such as that of Figure 5. The accumulation of nitroxide tends to introduce errors, and possibly some photodecomposition of TEMPO⁵⁸ occurs at the shorter wavelengths, with anticipated product accumulation in the single cell method. Overall, the multiple cell method is more reliable in this case.

The typical initiator used for LFRP benzoyl peroxide–styrene–TEMPO adduct **3** in essence is structurally similar to **1** with the exception of an additional benzoyl moiety. With this in mind, we anticipated that this system would be easily studied. It was expected that the TEMPO C–O cleavage (see eq 5) would lead to a

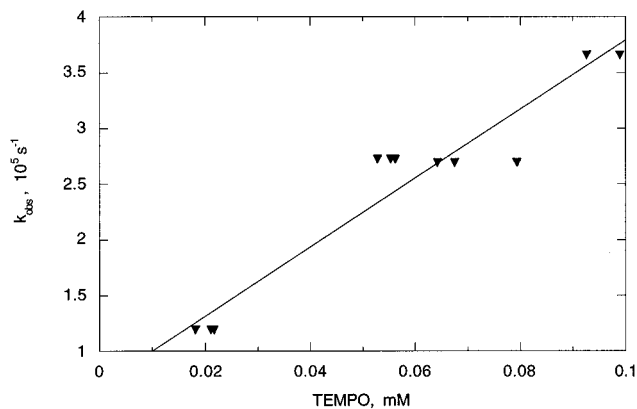


Figure 5. Quenching of methyl propionate radical with TEMPO monitored at 260 nm in acetonitrile using the multiple cell method.

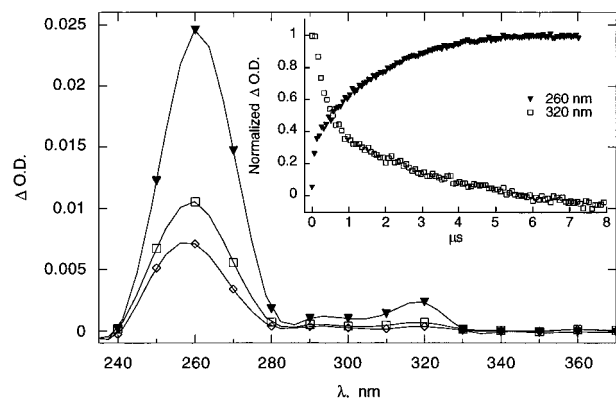
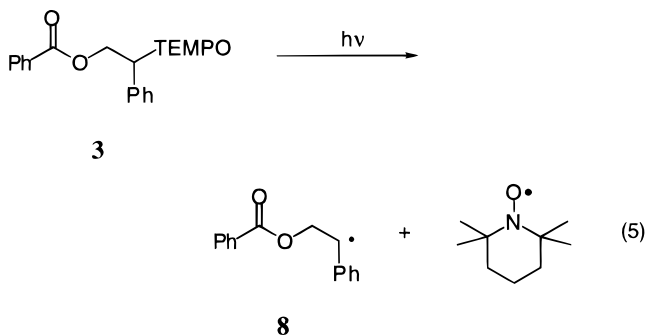


Figure 6. Transient spectrum of **3** in acetonitrile recorded 2.08 (▲), 9.04 (□), and 11.9 μ s (◇) after initial laser pulse. Inset: transients recorded after 266 nm excitation pulse with normalized Δ OD. Growth of transient (▼) monitored at 260 nm. Time scale is multiplied by 4. Decay of transient (□) recorded at 320 nm.

benzylic radical with significant absorption in the 320 nm region similar to the spectrum in Figure 1 for **1**. However, analysis of this commonly used initiator proved quite difficult, and the results of quenching are inconclusive due to the difficulty in assigning the transients in the spectrum obtained.



If the mechanism of eq 5 was the only important photochemical process, one would expect to observe essentially instantaneous formation of radical **8** followed by its decay. In other words, the study would follow closely the observations for the case of **1**. The spectrum recorded upon laser photolysis of **3** is shown in Figure 6; note that the two bands at 260 and ~ 320 nm decay with different kinetics and are appreciably different from **1**. From this figure it is clear that at least two

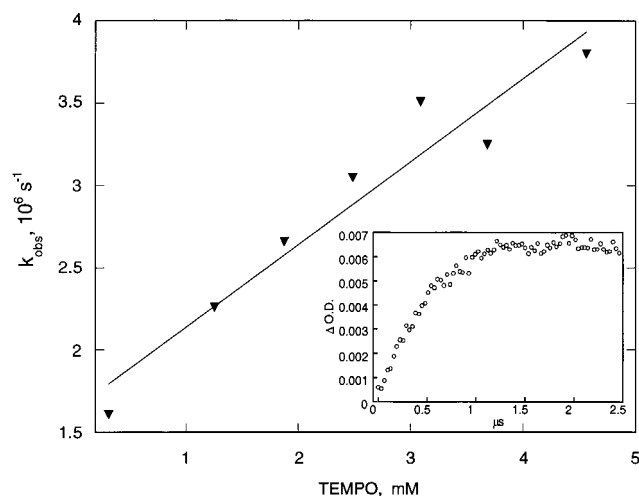
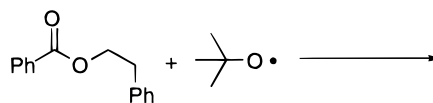


Figure 7. Quenching of **7** derived from **8** by TEMPO. Inset: growth of **8** monitored at 318 nm.

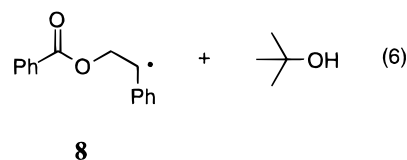
species are involved. In fact, a decay trace at 320 nm follows biexponential decay, suggesting that more than one species absorb at this wavelength. This is illustrated in the inset of Figure 6 that leads to lifetimes of 0.38 and 5.5 μs , with weights of essentially 50% each. To our surprise, at 260 nm we observe a signal growth in the 1.2 μs time scale. The kinetics for this growth is concurrent with the decay of the fast portion of the decay observed at 320 nm, thus suggesting that the short-lived 320 nm intermediate is the precursor of the 260 nm signal. The growth of the yet unidentified transient is illustrated in the inset of Figure 6. In cyclohexane, the kinetics at 260 and 320 nm also agree, and both are absent under oxygen saturation, suggesting the involvement of free radicals. The response to TEMPO addition is also different at the two wavelengths. At 320 nm TEMPO quenching leads to a bimolecular rate constant of $2.1 \times 10^9 \text{ M}^{-1} \text{ s}^{-1}$ for the fast component and $1.8 \times 10^8 \text{ M}^{-1} \text{ s}^{-1}$ quenching for the slow component of this absorption. Meanwhile, the growth at 260 nm gives rise to a rate constant of $9.2 \times 10^9 \text{ M}^{-1} \text{ s}^{-1}$ under identical quenching conditions. The slower rate constant for TEMPO quenching at 320 nm is assumed to be the desired rate constant because the order of magnitude is similar to other radicals. The faster component is probably due to quenching of an excited state by TEMPO as nitroxides are known to quench triplets with similar rate constants.⁵⁹

Product studies are difficult due to the instability of **3** to GC conditions. In any event, it is clear from HPLC that the products of photodecomposition of **3** include styrene, but not benzoic acid. It is possible that if benzoyloxyl radicals are formed, they will decarboxylate almost quantitatively in the inert solvent. At high conversions, the products identified by LC-MS are **1**, hydroxylamine, and minor amounts of styrene. The true amount of styrene produced may be greater since the ionization method used for this analysis is not ideal for olefin detection. In general, the photolysis of **3** leads to mixed decomposition, and it is uncertain as to what is being quenched by the nitroxide since TEMPO is known to quench triplets⁵⁹ and undergo electron transfer^{60,61} and radical trapping,⁷⁻⁹ in addition to hydrogen abstraction,^{62,63} albeit slower than the other processes. The unexpected photochemical behavior of **3** is the focus of a recent communication,⁶⁴ and its full investigation is currently in progress.⁶⁵

To determine the rate constant for TEMPO quenching of **3**, a model compound, **7**, was synthesized. The TEMPO-free analogue can give the desired radical by hydrogen abstraction of the α -hydrogen by the *tert*-butoxyl radical.⁴⁶ Simple photolysis of **7** at 266 nm yields transients that cannot be identified and implies the participation of the carbonyl group in complex photochemistry. However, 308 or 337 nm excitation gives no detectable transients, as expected, and allows for studies using the hydrogen abstraction method. Reaction of **7** with *tert*-butoxyl yields the desired substituted 1-phenylethyl radical **8** by hydrogen abstraction schematically represented by eq 6.



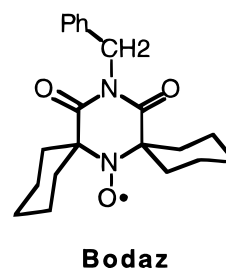
7



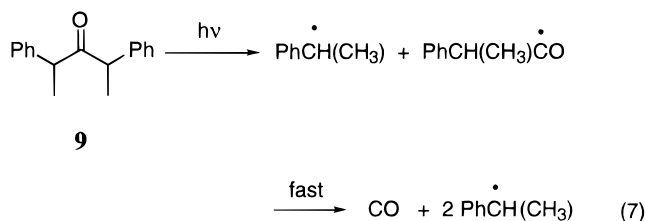
The spectra obtained by reaction with **7** and ethylbenzene are essentially identical and indicate that the desired benzylic radical is being generated. Since the signal of radical **8** derived from **7** by hydrogen abstraction was weak, it was thought that the abstraction could also occur at the β -position. Steady-state irradiation at 300 nm with 1.2 equiv of TEMPO and **7** dissolved in neat Bu^oOObu^t gave only **3**, confirmed by NMR. Therefore, α -abstraction occurs exclusively, albeit with a low efficiency.

The absence of the benzoyl moiety in compound **4** would lead one to believe that its direct photochemistry would be less complicated than that experienced with compound **3**. The transient absorption spectrum recorded in acetonitrile with 266 nm excitation did not yield the characteristic maxima ca. 319 and 305 nm, typical of the 1-phenylethyl radical. In lieu was a broad absorption band spanning from 270 to 350 nm, possibly a result of the secondary photochemistry involving the functionalities in the 3-, 4-, and 5-positions on the nitroxide moiety.

Similar to compound **3**, **4** seems to produce two transients which are indicated by the biexponential decay at 314 nm and a similar growth rate at 250 nm. The kinetics of these two species are identical within experimental error and suggest complex photochemistry. The 314 nm transient is quenched by Bodaz with a rate constant of $2.1 \times 10^9 \text{ M}^{-1} \text{ s}^{-1}$, too fast to involve a benzylic radical.



To circumvent this problem, the radical can be prepared by two alternate routes: hydrogen abstraction from 1 M solution of ethylbenzene gives the 1-phenylethyl radical where its decay can be monitored at 319 nm as a function of Bodaz concentration leading to a rate constant of $9.5 \times 10^7 \text{ M}^{-1} \text{ s}^{-1}$. The Norrish type I reaction gives better values than the hydrogen abstraction method because the latter is inherently slower due to the multistep reactions that are required to produce the 1-phenylethyl radical. Photolysis of **9** yields the radical rapidly and efficiently.^{29,66–69} Upon photolysis, α -cleavage occurs, giving rise to a 1-phenylethyl radical and an acyl radical that rapidly decarbonylates. The photoinduced decomposition of **9** is represented by eq 7.



The Norrish type I reaction of **9** was used in order to determine accurate quenching constants corresponding to the back-reaction leading to compounds **4** and **6**. In contrast with the di-*tert*-butyl peroxide method, the substituted ketone is a fast precursor of two 1-phenylethyl radicals,^{68,69} thereby leading to better rate constants for nitroxide trapping.

Compound **5** differed from the previous compounds in that it afforded the typical 1-phenylethyl radical by homolytic C–O bond cleavage by direct 266 nm excitation. The absorption spectrum of the radical gave the characteristic absorptions at 304 and 320 nm, and the decay of the latter was monitored as a function of nitroxide concentration. The rate constant obtained is similar to those obtained for related systems (see Table 2). The indirect method, as used for compound **4** using Bu'OO'Bu with ethylbenzene, was used to verify k_3 for compound **5** and led to a slightly slower rate constant, as usual. A rate constant was determined for the quenching the 1-phenylethyl radical derived from **9** by di-*tert*-butyl nitroxide. This value is identical to that derived from the direct method within experimental error.

The ketone method was also used to determine the rate constants for compound **6** as the benzoyl group on the nitroxide would lead to difficulties as encountered with **3**.

Discussion

The initiators that have been examined can be grouped into two major classes on the basis of the type of carbon-centered radical generated upon decomposition, aliphatic and aromatic. The pseudo-first-order experimental conditions used exclusively yield the rate constants for trapping of the carbon-centered radical by the nitroxide according to eq 3. The aromatic (1-phenylethyl) radicals are all quenched with rate constants around $10^8 \text{ M}^{-1} \text{ s}^{-1}$, which are well below diffusion control limit of $\sim 10^{10} \text{ M}^{-1} \text{ s}^{-1}$ for acetonitrile. However, the aliphatic radical derived from **2** is faster by an order of magnitude. This is mainly due to the carbon-centered radical structure and not because of the nitroxide structure. This is apparent from the measured

rate constants for **1** and **2** that differ by an order of magnitude and are different only in their carbon-centered radical structure. The rate constant for the trapping of the aliphatic radical is similar to that obtained by Ingold^{7–9} for the *n*-nonyl radical, and its fast kinetics reflects the lack of resonance stabilization compared with benzylic analogues (vide supra). The values measured by Ingold et al., shown in Table 1, are slower than our experimentally determined values simply because their analysis method involves the indirect (and consequently slower) formation of the radical under study, viz. reactions of *tert*-butoxy radicals. The values measured by direct photolysis are in general more accurate as the radical to be observed is generated within the laser pulse ($\sim 10 \text{ ns}$), and the rate-limiting step becomes the desired trapping reaction.

The fast rate of trapping for the acrylate probe provides some insight into the dynamics of the initial polymerization process and the problems in achieving living conditions with acrylate systems in general. This poor behavior is possibly due to a combination of detrimental factors. Typical polymerization temperatures (e.g., 125 °C) likely induce less decapping of the nitroxide group for acrylate systems, where the C–O bond is probably stronger than in benzylic systems.¹⁹ Any decapping that does occur will be rapidly reversed. A balance between polymerization temperature and steady-state nitroxide concentration must be found for acrylate systems to sustain living polymerization.

Taking **1** to be the benchmark for the other initiators, there appears to be little variation within the rates for the various nitroxide groups. This holds true when comparing the direct methods, when possible, with the radical derived from **9** which provides a convenient fast radical source. The rate constants observed are all within the upper $10^7 \text{ M}^{-1} \text{ s}^{-1}$ and lower $10^8 \text{ M}^{-1} \text{ s}^{-1}$ region. Comparing different nitroxides, only the rate constants for di-*tert*-butyl nitroxide appear to be marginally lower.

The rates of **6** and **1** are essentially identical within experimental error and suggest that substitution at the 4-position of the nitroxide does not play an important role for the stabilization or destabilization of the radical. Furthermore, the substituent at C-4, despite its bulkiness, is too far away to influence the kinetics.

The only factor that seems to influence the rate of trapping by nitroxide is the nature of the actual carbon-centered radical. This is seen between the rates of **2** compared to the other initiators studied. Also, the fast rate obtained for **2** is nearly 30 times faster than that for **1**, and the difference lies only with the type of radical generated.

In summary, the nonstabilized radicals such as that derived from **2** react with nitroxides much faster than do benzylic radicals. Nitroxide structure offers limited control of the reactivity for the trapping of the radical, but electronic effects may be a factor. Continuous photolysis of the initiators leads to some nitroxide accumulation and as a consequence reduced carbon-centered radical lifetime, pseudo-first-order decays, and dominant cross-termination reactions.

Acknowledgment. J.C.S. thanks the Natural Sciences and Engineering Research Council of Canada for support and the Instituto de Tecnología Química (Valencia) where this article was completed while J.C.S. was a guest under the auspices (Grant SAB1998-0121) of the

Ministerio de Educación y Ciencia (Spain). W.G.S. acknowledges NSERC for support through a graduate scholarship.

References and Notes

- (1) Nagashima, T.; Curran, D. P. *Synlett* **1996**, 4, 330.
- (2) Dagonneau, M.; Kagan, E. S.; Mikhailov, V. I.; Rozantsev, E. G.; Sholle, V. D. *Synthesis* **1984**, 11, 895.
- (3) Rychnovsky, S. D.; Vaidyanathan, R. *J. Org. Chem.* **1999**, 64, 310.
- (4) Cella, J. A.; Kelley, J. A.; Kenenhan, E. F. *Tetrahedron Lett.* **1975**, 33, 2869.
- (5) Limoges, B.; Degrand, C. *J. Electroanal. Chem.* **1997**, 422, 7.
- (6) Duz, A.; Onen, A.; Yagci, Y. *Makromol. Chem.* **1998**, 258, 1.
- (7) Bowry, V. W.; Ingold, K. U. *J. Am. Chem. Soc.* **1992**, 114, 4992.
- (8) Chateaufneuf, J.; Luszytyk, J.; Ingold, K. U. *J. Org. Chem.* **1988**, 53, 1629.
- (9) Beckwith, A. J.; Bowry, V. W.; Ingold, K. U. *J. Am. Chem. Soc.* **1992**, 114, 4983.
- (10) Rizzardo, E.; Solomon, D. H. *Polym. Bull.* **1979**, 1, 529.
- (11) Moad, G.; Rizzardo, E.; Solomon, D. H. *Macromolecules* **1982**, 15, 909.
- (12) Moad, G.; Rizzardo, E.; Solomon, D. H. *J. Macromol. Sci., Chem.* **1982**, A17, 51.
- (13) Moad, G.; Rizzardo, E.; Solomon, D. H. *Polym. Bull.* **1982**, 6, 589.
- (14) Solomon, D. H.; Rizzardo, E.; Cacioli, P. US Patent 4,581,429, 1986.
- (15) Georges, M. K.; Veregin, R. P. N.; Kazmaier, P. M.; Hamer, G. K. *Macromolecules* **1993**, 26, 2987.
- (16) Georges, M. K.; Veregin, R. P. N.; Kazmaier, P. M.; Hamer, G. K.; Saban, M. *Macromolecules* **1994**, 27, 7228.
- (17) Stevens, M. P. *Polymer Chemistry, An Introduction*, 2nd ed.; Oxford University Press: New York, 1990; p 633.
- (18) Hawker, C. J. *J. Am. Chem. Soc.* **1994**, 116, 11185.
- (19) Skene, W. G.; Belt, S. T.; Connolly, T. C.; Hahn, P.; Scaiano, J. C. *Macromolecules* **1998**, 31, 9103.
- (20) Baldovi, M. V.; Mohtat, N.; Scaiano, J. C. *Macromolecules* **1996**, 29, 5497.
- (21) Scaiano, J. C. *J. Am. Chem. Soc.* **1980**, 102, 7747.
- (22) Scaiano, J. C.; Tanner, M.; Weir, D. *J. Am. Chem. Soc.* **1985**, 107, 4396.
- (23) Matyjaszewski, K.; Woodworth, B. E.; Zhang, X.; Gaynor, S. G.; Metzner, Z. *Macromolecules* **1998**, 31, 5955.
- (24) Hawker, C. J.; Barclay, G. G.; Orellana, A.; Dao, J.; Devonport, W. *Macromolecules* **1996**, 29, 5245.
- (25) Hawker, C. J.; Barclay, G. G.; Dao, J. *J. Am. Chem. Soc.* **1996**, 118, 11467.
- (26) Ramey, C. E.; Luzzi, J. J. U.S. Patent 3,936,456, 1976.
- (27) Benoit, D.; Chaplinski, V.; Braslau, R.; Hawker, C. J. *J. Am. Chem. Soc.* **1999**, 121, 3904.
- (28) Baretz, B. H.; Turro, N. J. *J. Am. Chem. Soc.* **1983**, 105, 1309.
- (29) Turro, N. J. *Modern Molecular Photochemistry*; University Science Books: Sausalito, 1991; p 628.
- (30) Skene, W. G.; Scaiano, J. C. *J. Phys. Chem.*, in press.
- (31) Skene, W. G. Unpublished work.
- (32) Laidler, K. J.; Meiser, J. H. *Physical Chemistry*; The Benjamin/Cummings Publishing Company, Inc.: Menlo Park, CA, 1982; p 919.
- (33) Lowry, T. H.; Richardson, K. S. *Mechanism and Theory in Organic Chemistry*, 3rd ed.; Harper Collins Publishers: New York, 1987; p 1090.
- (34) Fischer, H. *Macromolecules* **1997**, 30, 5666.
- (35) Fischer, H. *J. Am. Chem. Soc.* **1986**, 108, 3925.
- (36) Beckwith, A. L. J.; Bowry, V. W.; O'Leary, M.; Moad, G.; Rizzardo, E.; Solomon, D. H. *J. Chem. Soc., Chem. Commun.* **1986**, 1003.
- (37) Catala, J. M.; Bubel, F.; Hammouch, S. O. *Macromolecules* **1995**, 28, 8441.
- (38) Veregin, R. P. N.; Georges, M. K.; Hamer, G. K.; Kazmaier, P. M. *Macromolecules* **1995**, 28, 4391.
- (39) Howell, B. A.; Priddy, D. B.; Li, I. Q.; Smith, P. B.; Kastl, P. E. *Polym. Bull.* **1996**, 37, 451.
- (40) Steenbock, M.; Klapper, M.; Mullen, K.; Pinhal, N.; Hubrich, M. *Acta Polym.* **1996**, 47, 276.
- (41) Greszta, D.; Matyjaszewski, K. *Macromolecules* **1996**, 29, 7661.
- (42) Connolly, T. J.; Baldovi, M. V.; Mohtat, N.; Scaiano, J. C. *Tetrahedron Lett.* **1996**, 37, 4919.
- (43) Scaiano, J. C.; Connolly, T. J.; Mohtat, N.; Pliva, C. N. *Can. J. Chem.* **1997**, 75, 92.
- (44) Korolenko, E. C.; Cozens, F. L.; Scaiano, J. C. *J. Phys. Chem.* **1995**, 99, 14123.
- (45) Chatgililoglu, C. In *Handbook of Organic Photochemistry*; Scaiano, J. C., Ed.; CRC Press: Boca Raton, FL, 1989; Vol. II, p 3.
- (46) Paul, H.; Small, R. D., Jr.; Scaiano, J. C. *J. Am. Chem. Soc.* **1978**, 100, 4520.
- (47) Chong, Y. K.; Ercole, F.; Moad, G.; Rizzardo, E.; Thang, S. H.; Anderson, A. G. *Macromolecules* **1999**, 32, 6895.
- (48) Odell, P. G.; Rabien, A.; Michalak, L. M.; Vergin, R. P. N.; Quinlan, M. H.; Moffat, K. A.; MacLeod, P. J.; Listigovers, N. A.; Honeyman, C. H.; Georges, M. K. *Polym. Prepr.* **1997**, 38, 414.
- (49) Georges, M. K.; Listigovers, N. A.; Odell, P. G.; Hamer, G. K.; Quinlan, M. H.; Veregin, R. P. N. *Polym. Prepr.* **1997**, 38, 454.
- (50) MacLeod, P. J.; Georges, M. K.; Quinlan, M.; Moffat, K. A.; Listigovers, N. A. *Polym. Prepr.* **1997**, 38, 459.
- (51) Keoshkerian, B.; Georges, M.; Quinlan, M.; Veregin, R.; Goodbrand, B. *Macromolecules* **1998**, 31, 7559.
- (52) Goto, A.; Fukuda, T. *Macromolecules* **1999**, 32, 618.
- (53) O'Neil, G. A.; Torkelson, J. M. *Macromolecules* **1999**, 32, 411.
- (54) Rizzardo, E.; Serelis, A. K.; Solomon, D. H. *Aust. J. Chem.* **1982**, 35, 2013.
- (55) de Leon, M. E.; Gnanou, Y.; Guerrero, R. *Polym. Prepr.* **1997**, 38, 667.
- (56) A recent radiolytic study of the reaction of methyl methacrylate with OH radicals in aqueous solution observed similar signals: Wojnárovits, L.; Takács, E. *Res. Chem. Intermed.* **1999**, 25, 275.
- (57) Lambert, J. B.; Shurvell, H. F.; Lightner, D.; Cooks, R. G. *Introduction to Organic Spectroscopy*; Macmillan Publishing Company: New York, 1987; p 454.
- (58) Johnston, L. J.; Tencer, M.; Scaiano, J. C. *J. Org. Chem.* **1986**, 51, 2806.
- (59) Lissi, E. A.; Encinas, M. V. In *Handbook of Organic Photochemistry*; Scaiano, J. C., Ed.; CRC Press: Boca Raton, FL, 1989; Vol. 2, p 111.
- (60) Green, S.; Fox, M. A. *J. Phys. Chem.* **1995**, 99, 14752.
- (61) Rozantsev, E. G.; Sholle, V. D. *Synthesis* **1971**, 401.
- (62) Scaiano, J. C. *Chem. Phys. Lett.* **1981**, 79, 441.
- (63) Connolly, T. J.; Scaiano, J. C. *Tetrahedron Lett.* **1997**, 38, 1133.
- (64) Skene, W. G.; Scaiano, J. C. *Polym. Prepr.* **2000**, 41, 163.
- (65) Skene, W. G.; Scaiano, J. C. Manuscript in preparation.
- (66) Engel, P. S. *J. Am. Chem. Soc.* **1970**, 92, 6074.
- (67) Robbins, W. K.; Eastman, R. H. *J. Am. Chem. Soc.* **1970**, 92, 6076.
- (68) Turro, N. J.; Gould, I. R.; Baretz, B. H. *J. Phys. Chem.* **1983**, 87, 531.
- (69) Lunazzi, L.; Ingold, K. U.; Scaiano, J. C. *J. Phys. Chem.* **1983**, 87, 529.

MA991753C